



CHAPTER 3

Materials, methods, and characterization techniques

The methodologies for sample preparation, fabrication, and characterization techniques have been covered in this chapter. Graphene oxide was successfully synthesized using the modified Hummers method by taking natural graphite flake powder as a raw material. PANI was synthesized by the COP method. The combustion approach was used to create all the metal oxides, including copper cobaltite, copper ferrite, and cobalt ferrite.

As a component of carbonaceous materials, graphene and its derivatives have been regarded as new materials. Due to its unique physicochemical characteristics, which include a high specific surface area, robust mechanical strength, superior thermal conductivity, extraordinary optical transmittance, and electron transport capabilities, it has a significant impact on the field of electrochemistry. Graphite is subjected to an oxidation process to produce graphite oxide, which is then dispersed and delaminated in water or other suitable organic solvents to create GO. However, dried, agglomerated forms of GO can also be used or stored. The numerous hydroxyl and epoxide groups on the basal plane and the carboxylic groups at the sheet edges are known to make up the majority of GO's chemical structure. Intriguing physicochemical characteristics, such as electrical, optical, thermal, mechanical, and electrochemical capabilities, as well as chemical reactivity, are conferred to GO by the presence of oxygen functional groups. For the purpose of chemically modifying or functionalizing GO, these oxygen functional groups can work as efficient immobilization sites for various electroactive species. So GO's physicochemical characteristics can be adjusted chemically, thermally, or electrochemically. There are very few researches where graphene oxide is taken as a carbon material source. So, we have taken graphene oxide as a carbon-based material and we have not used any filler separately [181–183]. PANI has been taken due to its availability, cost, ease of synthesis, and high conducting nature than other

conducting polymers like PPy, PTh, etc. In the subject of supercapacitors, extensive study has been done on transition metal oxides such as cobalt oxide, copper oxide, iron oxide, etc. In order to benefit from several oxidation states (from both metals) from a single molecule, we have synthesized bimetallic oxides such as copper cobaltite (combination of Cu and Co), copper ferrite (combination of Cu and Fe), and cobalt ferrite (combination of Co and Fe) [184].

The synthesized materials were investigated in-depth using two methods of characterization: material characterization and electrochemical characterization. In material characterization, XRD, FTIR, FESEM, and EDS were performed. In electrochemical characterization, we performed CV, CD, and EIS.

3.1. Materials

Sulfuric Acid, hydrochloric acid, hydrogen peroxide, aniline, 2-propanol, carbon paper, silver conductive adhesive paste, and nafion solution were bought by Alfa Aesar. Graphite synthetic (Type 3) C, KMnO_4 (Potassium permanganate), NaNO_3 (Sodium Nitrate), PTSA (Toluene-4-Sulphonic Acid), APS (Ammonium peroxodisulphate), copper nitrate, aminoacetic acid (Glycine), ferric nitrate, cobalt nitrate, and other required chemicals were purchased from SRL, India. All materials are around 99.99% pure (ACS category) and used without any further processing. All the experiments were performed by using double distilled water as solvent. Chemical properties of the chemical compounds have been given in table 3.1.

Table 3.1: Specifications of the chemical compounds

Name	Chemical formulae	Molar mass (g/mol)	Solubility in water at 20-25 °C (g/mL)
Hydrochloric acid	HCl	36.45	Soluble
Sulphuric acid	H ₂ SO ₄	98.07	Soluble
Hydrogen peroxide	H ₂ O ₂	34.01	Miscible
Potassium permanganate	KMnO ₄	158.03	5/100
Sodium nitrate	NaNO ₃	84.99	91.2/100
Aniline	C ₆ H ₇ N	93.13	Insoluble
PTSA	C ₇ H ₈ O ₃ S.H ₂ O	190.22	67/100
APS	(NH ₄) ₂ S ₂ O ₈	228.2	80/100
Copper nitrate	Cu(NO ₃) ₂ .3H ₂ O	241.6	267/100
Ferric nitrate	Fe(NO ₃) ₃ .9H ₂ O	404	150/100
Cobalt nitrate	Co(NO ₃) ₂ .6H ₂ O	291.04	66.96/100
Glycine	C ₂ H ₅ NO ₂	75.07	25/100

3.2. Synthesis procedure

3.2.1. Synthesis of graphene oxide

Modified hummer's method was used to synthesize GO [185]. Graphite flake powder (2.0 g) and sodium nitrate solids (2.0 g) were put into the beaker having 90 mL of H₂SO₄ (98%). The beaker was put on a magnetic stirrer for 4 hours followed by continuous stirring under

an ice bath and the temperature was maintained below 5 °C. After 4 hours, 12 g KMnO_4 was slowly added into the mixture with constant stirring (figure 3.1). The mixture was removed from the ice bath and temperature was maintained at 35 °C with 2 hours stirring. After the mixture became a little waxy, 180 mL DDW was slowly mixed and stirred for about an hour. The solution was heated around 95 °C for 1 hour, with constant stirring. The mixture was then left for cooling at room temperature. 100 mL of DDW was again added with continuous stirring for about an hour. 30% H_2O_2 (5 mL) was added to the mixture, the color changed to dark yellow. The mixture was then centrifuged, washed several times with 10% HCl solution and DDW, to remove the unwanted metal ions. Lastly, the resulted product was dried in a vacuum oven at 120 °C overnight.

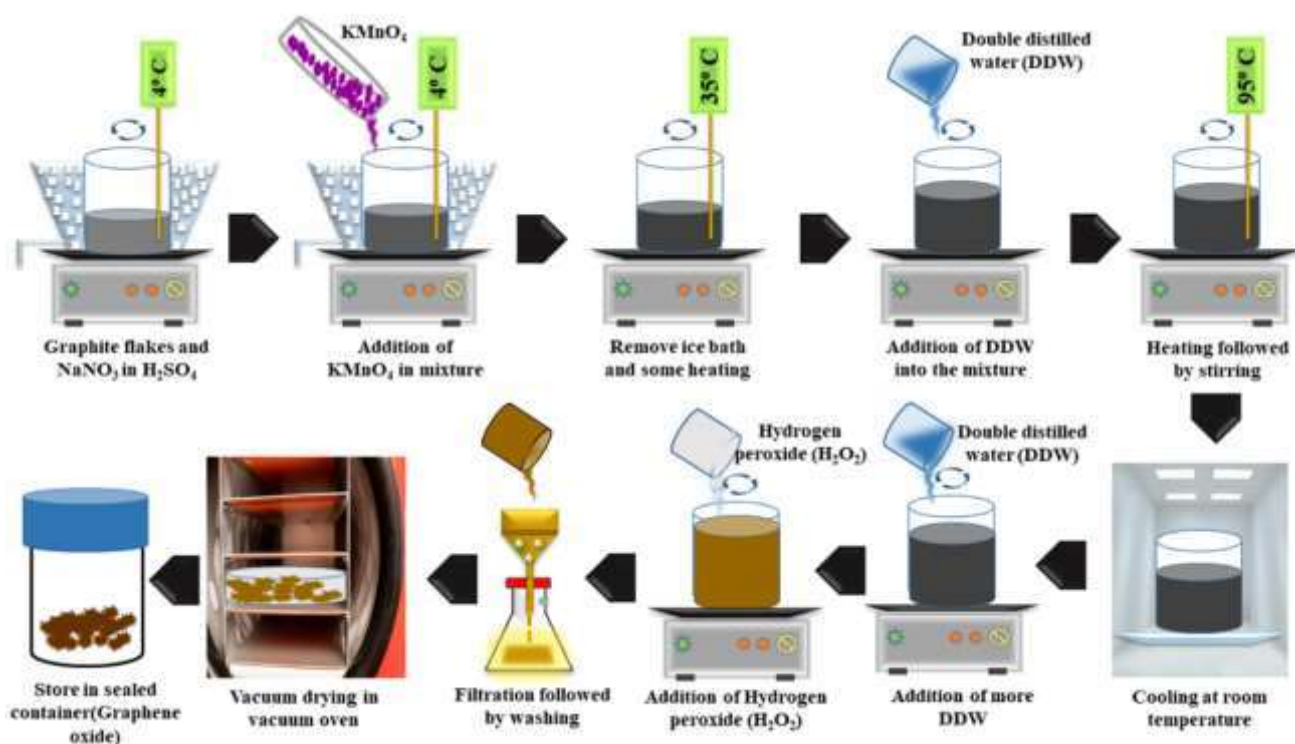


Figure 3.1: Schematic diagram of GO synthesis via modified hummer's method

3.2.2. Synthesis of polyaniline

PANI was synthesized from aniline monomer by COP reaction. APS acted as an initiator and oxidant. PTSA was taken as dopant. 5 mL of aniline was taken for preparing the sample. Desired amount of PTSA and APS were completely dissolved in double distilled water separately and kept at 2 °C along with aniline of required quantity. Furthermore, 1M PTSA and 1M APS solution were prepared in double distilled water. Ice bath was used to maintain the temperature at 2 °C throughout the process. Initially, aniline was released dropwise into the previously prepared PTSA solution followed by stirring for 1 hour. The resulting solution was stirred continuously to prevent precipitation and maintaining homogeneity. To initiate the polymerization reaction, APS solution was added very slowly to the aniline-PTSA solution. This polymerization process is exothermic in nature; so, a very slow addition of APS was done to prevent any abrupt rise in temperature [186–188]. Initially the solution was brownish in colour, eventually a dark green precipitate was formed on complete addition of APS solution. The resulting mixture (precipitate) was stirred for 1 hour, kept in a refrigerator overnight followed by vacuum filtration and vacuum drying at 60 °C for 5 hours (figure 3.2, 3.3 and 3.4). The dried samples were ground to powder form and stored at normal conditions for further use.

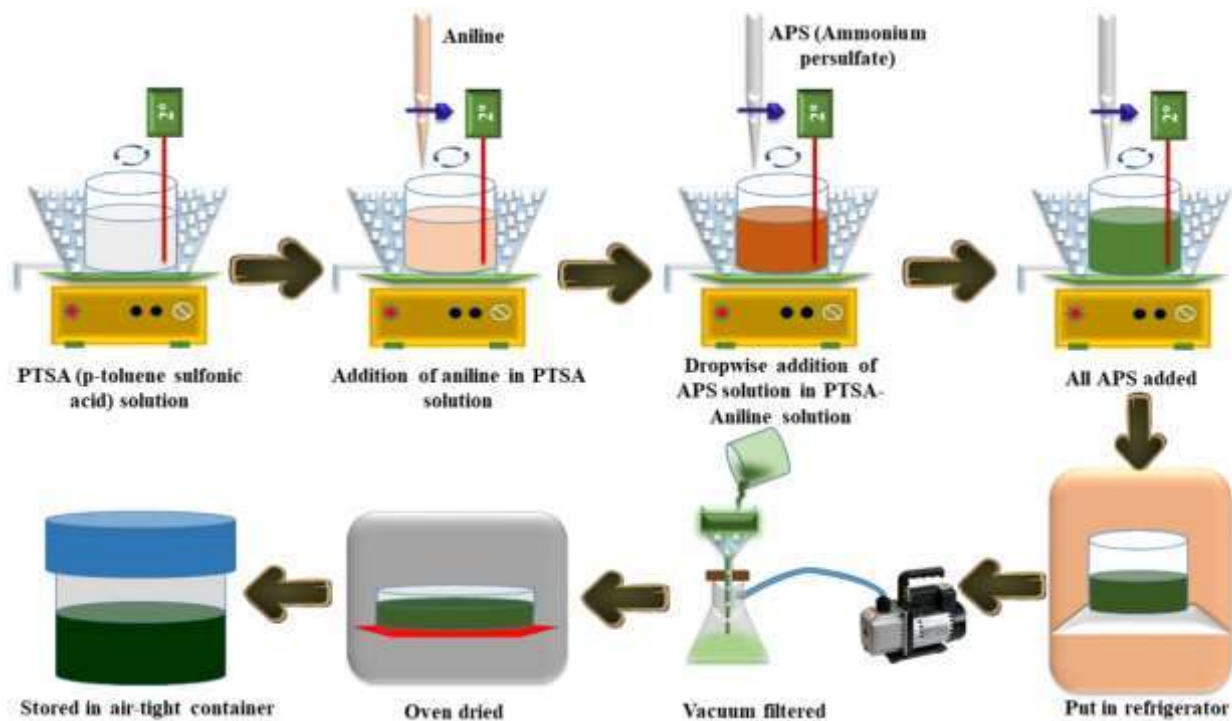


Figure 3.2: Schematic diagram of experimental set-up

If all the aniline is added to PTSA instantly, then the temperature will rise and very low-grade polyaniline will be formed.

If all the APS is added at a time, the sample will burn due to uncontrollable and highly exothermic reaction.

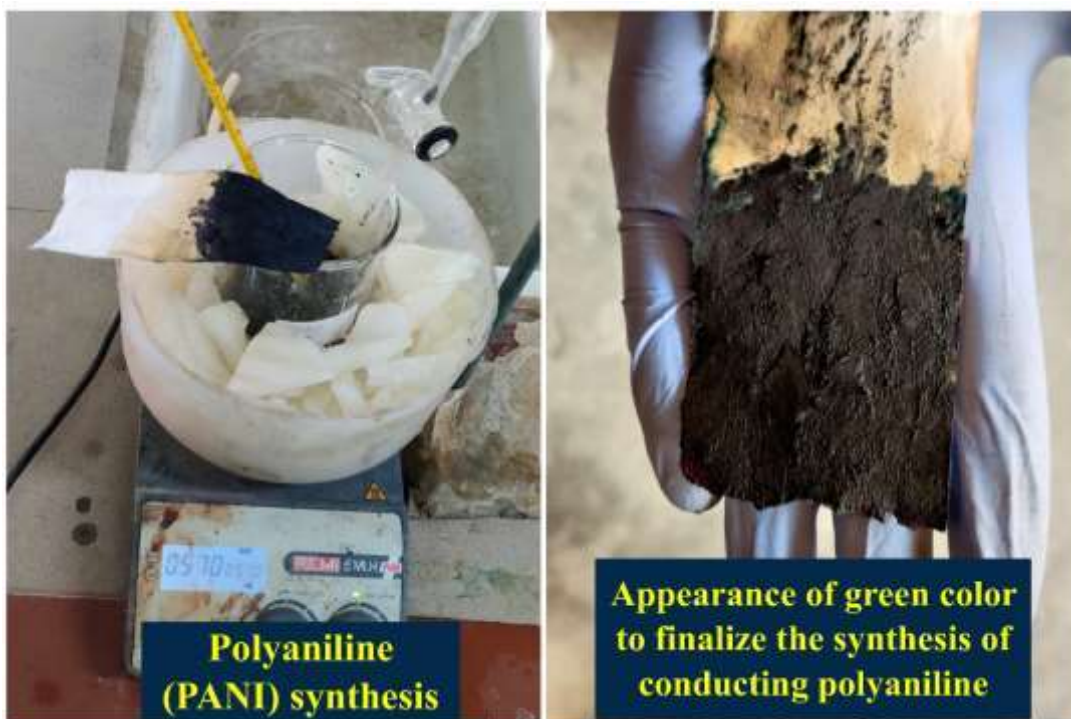


Figure 3.3: Experimental set-up used in the laboratory for the synthesis of PANI

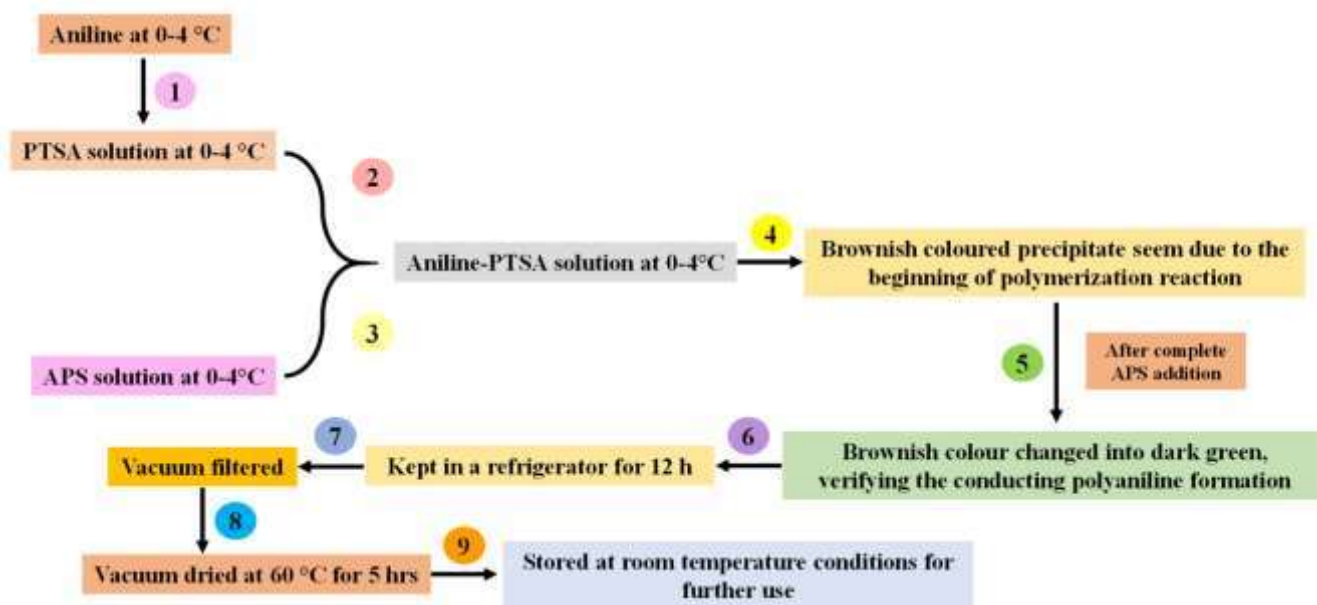
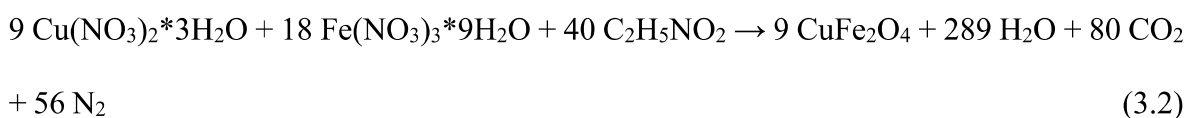
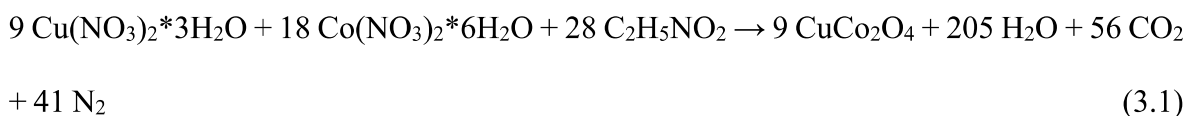


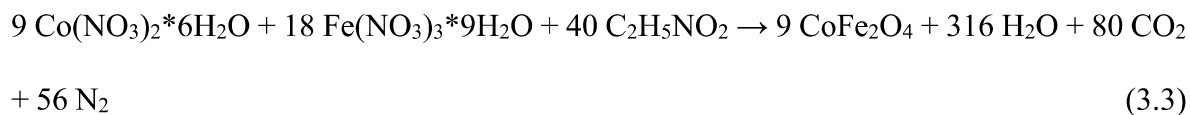
Figure 3.4: Flow sheet of the synthesis of polyaniline

3.2.3. Synthesis of metal oxides

Solution combustion technique was used to synthesize all the metal oxides. The schematic and practical set up for the preparation of metal oxides have been shown in figure 3.5, 3.6 and 3.7. For the synthesis of copper cobaltite, copper and cobalt nitrates having molar ratio of 1:2 were dissolved in 500 mL of DDW followed by the addition of glycine as a fuel (equation 3.1). The final solution was heated at 80 °C followed by stirring for around 8-9 hours. Eventually water evaporated and auto combustion started with the formation of gases due to the exothermic reactions created by the fuel (glycine). After complete combustion, foam shaped binary metal complexes were obtained [189]. They were then ground to fine powder and uncalcined copper cobaltite was obtained. Uncalcined copper cobaltite was calcined at 800 °C to get crystalline and pure phase of copper cobaltite [calcined copper cobaltite].

Other metal oxides were also prepared following the same procedure. Equation 3.2 and 3.3 represents the stoichiometric proportions of the corresponding precursors for the synthesis of the copper ferrite and cobalt ferrite, respectively [190,191]. Uncalcined copper ferrite was calcined at 800 °C to get crystalline copper ferrite. Similarly, calcined cobalt ferrite was prepared by the calcination of as synthesized cobalt ferrite complex (uncalcined cobalt ferrite) at 800 °C. Table 3.2 contains all the information about the synthesis of metal oxides.



**Table 3.2:** Specifications of precursors used to synthesize metal oxides

Sample name	Precursors used (g)	Molar ratio	Calcination temperature (°C)
CuCo ₂ O ₄	Cu(NO ₃) ₂ ·3H ₂ O = 9.66	Cu:Co = 1:2	800
	Co(NO ₃) ₂ ·6H ₂ O = 23.28		
	Glycine = 9.36		
CuFe ₂ O ₄	Cu(NO ₃) ₂ ·3H ₂ O = 7.24	Cu:Fe = 1:2	800
	Fe(NO ₃) ₃ ·9H ₂ O = 24.24		
	Glycine = 10.13		
CoFe ₂ O ₄	Co(NO ₃) ₂ ·6H ₂ O = 8.73	Co:Fe = 1:2	800
	Fe(NO ₃) ₃ ·9H ₂ O = 24.24		
	Glycine = 10.13		

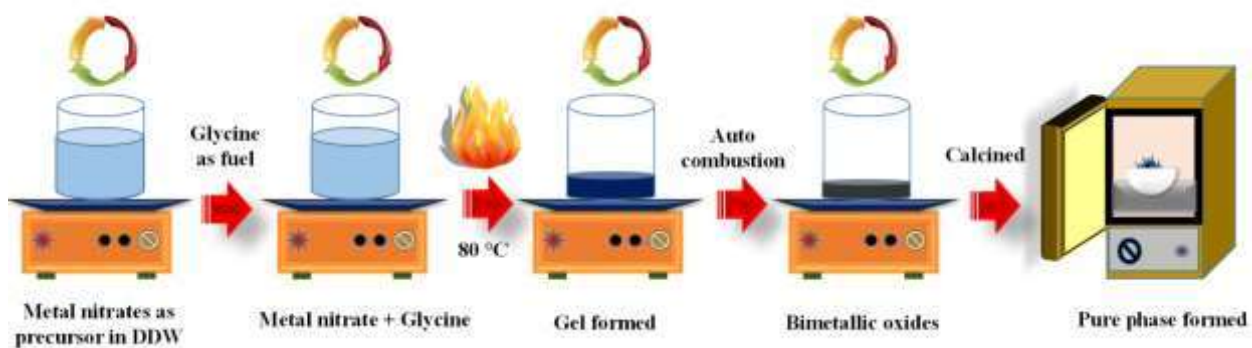


Figure 3.5: Schematic diagram of experimental set-up of metal oxides

Combustion synthesis process is highly exothermic in nature. Temperature of the hot plate/magnetic stirrer should not be more than 100 °C, otherwise amount of gas formed will be quite high that will throw the material outside. Slow and steady combustion process must be followed. Proper distance from the setup should be maintained during the combustion process.



Figure 3.6: Experimental set-up used in the laboratory to synthesize metal oxides

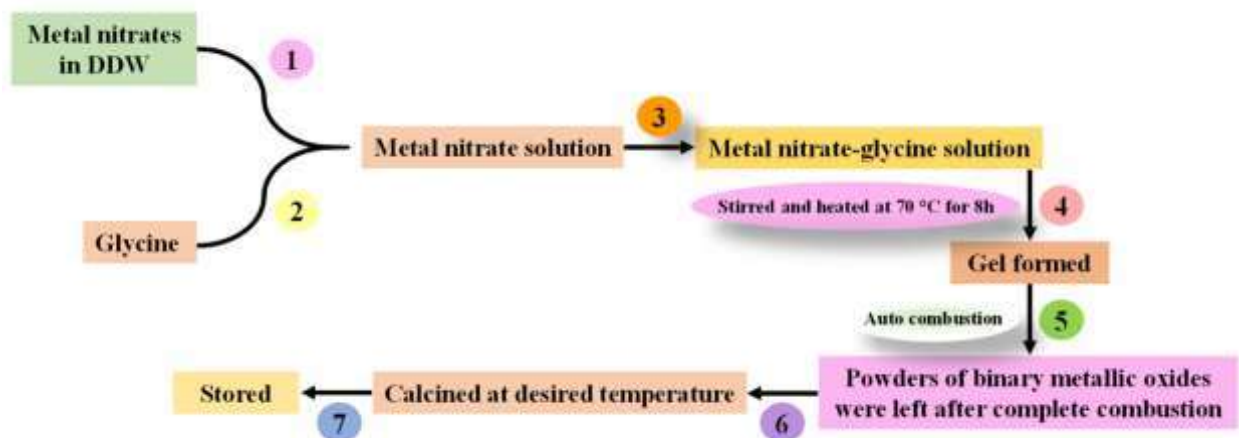


Figure 3.7: Flowsheet of the synthesis of metal oxides

3.2.4. Synthesis of GO and PANI based binary composite

Required amount of GO was dispersed in DDW and the dispersion was added to aniline-PTSA solution (table 3.3). Then, composite of GO-PANI was prepared by following the subsequent synthesis steps of polyaniline (figure 3.8, 3.9). In the similar way, binary composites of polyaniline and metal oxides (MO) were prepared (table 3.3). For the synthesis of polyaniline based binary composites, calcined metal oxides were used.

Table 3.3: Experimental details of the synthesis of polyaniline based binary composites

Sample name	Existing materials	Weight ratio of GO:Aniline or Aniline:MOx	Quantity of materials (mL or g)
GO/PANI	Graphene oxide and polyaniline	1:4	GO = 2.325 g Aniline = 9.12 mL
PANI/CuCo ₂ O ₄	Polyaniline and copper cobaltite	4:1	Aniline = 9.12 mL CuCo ₂ O ₄ = 2.325 g

PANI/CuFe ₂ O ₄	Polyaniline and copper ferrite	4:1	Aniline = 9.12 mL CuFe ₂ O ₄ = 2.325 g
PANI/CoFe ₂ O ₄	Polyaniline and cobalt ferrite	4:1	Aniline = 9.12 mL CoFe ₂ O ₄ = 2.325 g

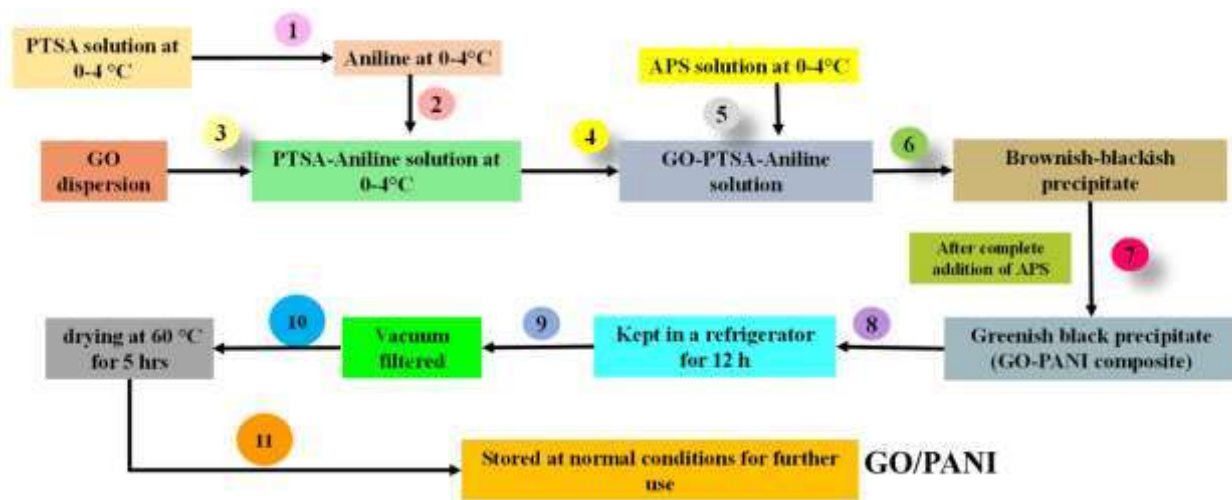


Figure 3.8: Flowsheet of the synthesis of binary composite GO/PANI

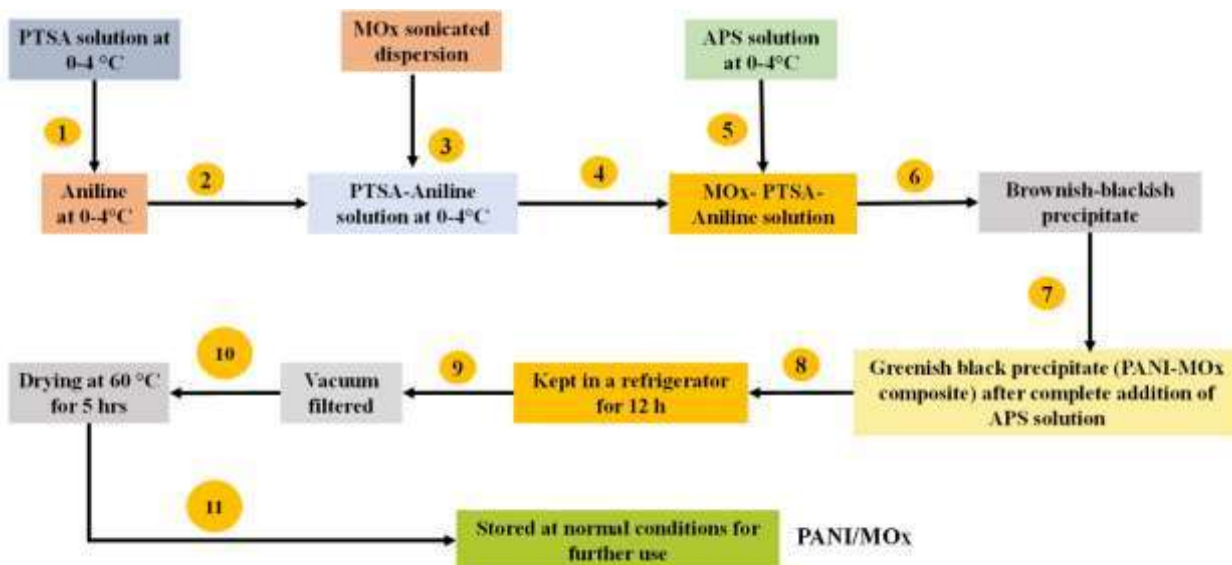


Figure 3.9: Flowsheet of the synthesis of binary composite PANI/MO_x**3.2.5. Synthesis of ternary composites**

Stoichiometric quantity of GO and MO_x (Copper cobaltite, copper ferrite, cobalt ferrite) were dispersed in double distilled water and then added to PTSA-Aniline solution before the initiation of polymerization reaction (as per table 3.4). Then APS was added dropwise to the PTSA-Aniline-GO-MO_x solution and the subsequent synthesis procedure of polyaniline was followed to prepare ternary composite (figure 3.10). Experimental data of all the ternary systems have been provided in table 3.4. For the synthesis of polyaniline based ternary composites, calcined metal oxides were used.

Table 3.4: Experimental data for ternary systems

Sample name	Weight ratio of GO:Aniline:MO _x	GO (g)	Aniline (mL)	MO _x (g)
GO/PANI/CuCo ₂ O ₄	1:4:1	2.325	9.12	2.325
GO/PANI/CuFe ₂ O ₄	1:4:1	2.325	9.12	2.325
GO/PANI/CoFe ₂ O ₄	1:4:1	2.325	9.12	2.325

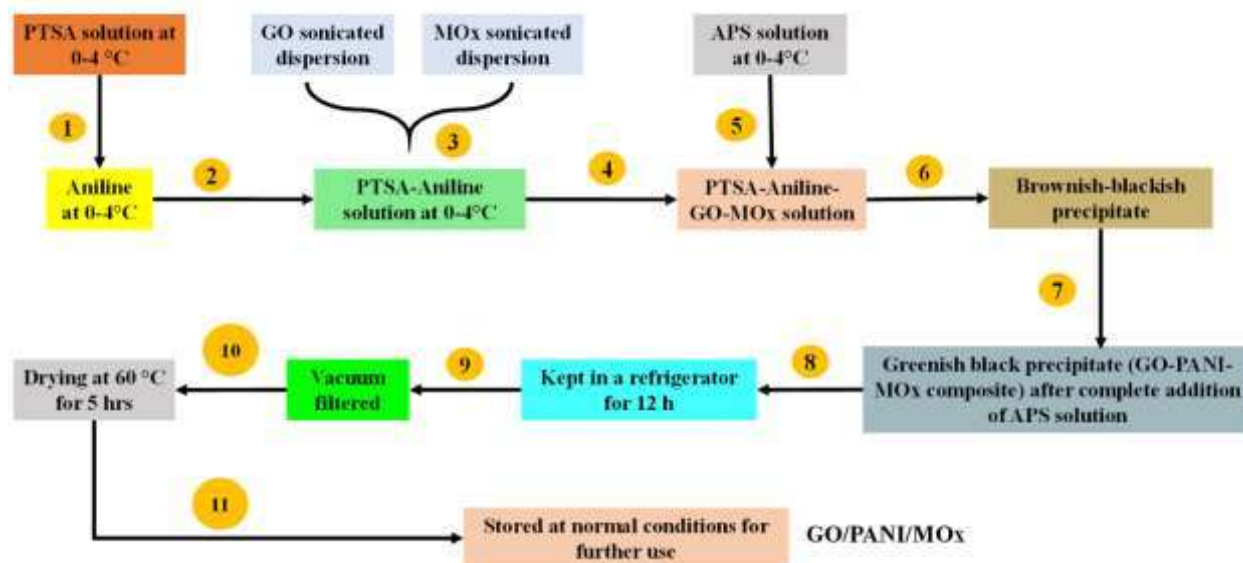


Figure 3.10: Flowsheet of the synthesis of ternary composites

3.2.6. Fabrication of electrodes and supercapacitors

The conducting substrate was coated with a slurry of synthetic materials, including conductive fillers (graphene oxide, carbon black, acetylene black, metal particles, graphite, etc.), binder (Nafion, PTFE, PVDF, SPEEK, etc.), and solvent (ethanol, water, NMP, DMSO, etc.). Understanding the significance of employing binders and conductive fillers when fabricating electrodes is crucial [192,193]. Supercapacitors endure a significant volume shift in their electroactive species during charging and discharging. The species may become detached from the substrate due to a volume change, however, binders will prevent that from happening, helping to prolong the cycle life. Electrical responses of conductive polymer composites are improved by conductive networks of conductive fillers. The tunneling between nearby conductive fillers dispersed throughout the polymer matrix, according to numerous researchers, causes conductive fillers to enhance the system's overall resistances [194]. Conductive polymers have been classified as intrinsically conductive

polymers and conductive polymer composite. Intrinsically conductive polymers don't require conductive fillers as electron transport is favored by their electronic structure. Conductive polymer composites require conductive fillers which turn on the conducting ability of insulating polymer matrix. However, if the conducting polymer-based composite is consisting of electrically conducting components (other than conductive polymer), then it is better to avoid excessive use of conductive fillers as it may increase the resistance, cost, and loss of flexibility of the base material [195,196].

In the present experimental set up, copper wire was taken as the current collector and a substrate (carbon paper) was attached to the copper wire with the help of silver conductive adhesive paste. Back side of the carbon paper and the exposed part of the copper wire were insulated by using gluestick. A dispersion was prepared by mixing 10 mg of the synthesized material (active material), 2-propanol (0.4 mL), nafion (15 μ L), and certain amount of the slurry (as per the desired active mass loading) was drop casted on the carbon paper of 1 cm² area. The prepared electrode was dried for around half an hour in a vacuum oven till complete disappearance of the used solvents [197]. Active material is Graphene oxide or polyaniline or metal oxide or any composite

Symmetric systems of two equal electrodes (working electrode having same mass loading and capacitance), whatmann filter paper as separator, and KOH electrolyte were assembled and put in a plastic casing to fabricate supercapacitors [198]. The fabricated electrodes were used in the supercapacitors. Some key points during electrode synthesis are given below:

(i) The targeted end of copper wire which must be connected to the carbon paper, flattened properly to avoid lose electrical connection.

(ii) Very small amount of silver paste must be applied to attach the copper wire, otherwise silver paste may get soaked on the other side of carbon paper (on the side where we will drop cast the prepared slurry) and give abrupt results.

(iii) Working, reference, counter electrode must be connected to their corresponding leads of the electrochemical cell, otherwise the instrument will show “power amplitude overload”.

(iv) While assembling the supercapacitor, the separator (here, whatmann filter paper) should not be having any wear and tear, and there must not be any direct physical contact between the electrodes.

(v) The stability potential window of the system must be found out by performing repeated cyclic voltammetry cycles.

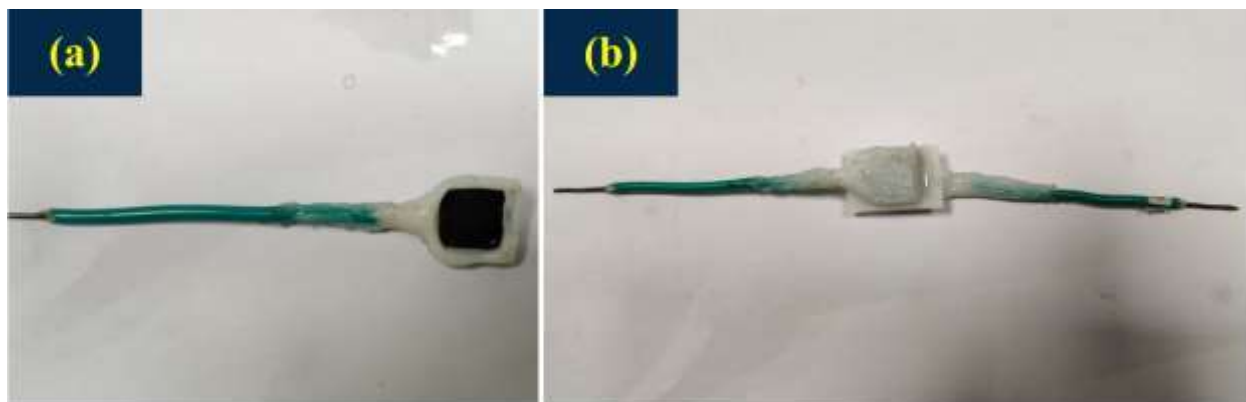


Figure 3.11: Fabricated (a) electrode and (b) supercapacitor

3.2.7. Characterization techniques

Table 3.5: Characterization techniques used in the present study

SI No.	Characterization technique	Characteristics studied

1.	XRD	Phase identification
2.	FTIR	Functional group analysis
3.	FESEM	Surface morphology of the samples
4.	EDS	Elemental analysis
5.	CV	Stable potential window determination, voltage-current relation, specific capacitance calculation
6.	CD	Determination of charging and discharging time, specific capacitance, coulombic efficiency, specific energy and power
7.	EIS	Charge transfer resistance, variation of net impedance, admittance, and capacitance with frequency, Knee frequency

3.2.8. Material characterization

3.2.8.1. XRD

XRD technique was used to identify the phase of the synthesized samples. XRD patterns of all the samples were obtained by using Cu K α radiation having wavelength (λ) of 1.54 Å with the help of an X-ray powder diffractometer (Benchtop-Rigaku Miniflex) in the range of 10° to 80°. The applied current and voltage were 200 mA and 40 kV, respectively. The calculated d-values were matched with the standard data of the corresponding JCPDS files

and the existing phases were identified. The crystallite size of the synthesized material was estimated by Scherrer's equation.

$$L = \frac{K\lambda}{FWHM \cos\theta} \quad (3.4)$$

L is the average crystallite size, λ is the X-ray wavelength (1.54056 Å), θ is the Bragg angle. K is the Scherrer's constant (we have taken 0.9 for spherical particle and 0.94 for nanorods). FWHM represents the full width at half maximum in radians, respectively.

3.2.8.2. FTIR

In FTIR, the functional groups are identified depending upon various vibration modes of the respective groups. Each sample was mixed with KBr (binder) to make pellet. Then, FTIR spectra were recorded by Nicolet iS5-Thermo electron scientific instruments LLC spectrophotometer in IR range of 4000-400 cm^{-1} for 64 scans at a resolution of 4 cm^{-1} . The data has been reported in the form of wavenumber vs transmittance.

3.2.8.3. FESEM and EDS

Nova Nano SEM 450 (FEI company of USA (S.E.A) PTE, LTD) was used to study the surface morphology of the synthesized samples by FESEM. The instrument was operated under vacuum and voltage of 1 kV. Various images were captured at different working distances and resolutions to get detailed information about the surface morphology. Team Pegasus Integrated EDS-EBSD with octane plus and Hikari Pro equipped with the FESEM machine was used to determine elemental percentages of the constituents by EDS.

3.2.8.4. Electrochemical characterization and performance evaluation of the fabricated systems

Performances of the supercapacitor electrodes are evaluated by various electrochemical techniques like CV, CD, and EIS. Specific capacitance (F/g), energy density (Wh/kg), power density (W/kg), coulombic efficiency (%), cycle life (% retention), impedance are the factors which determine the efficacy of electrochemical supercapacitors and supercapacitor electrodes. All the electrochemical characterization has been done at 20 °C temperature.

Various types of electrodes are used in the electrochemical measurements, such as, working electrode (WE), sense electrode (SE), reference electrode (RE), counter electrode (CE), and ground electrode (GE). VersaSTAT3 was used for all the measurements. Working electrode is the electrode at which probable reactions occur. Sense electrode is connected to the working electrode, and it controls the voltage in between the reference electrode and itself. Similarly, the voltage between reference electrode and sense electrode is measured by reference electrode. The role of counter electrode is to control the VersaSTAT3 power output. Ground lead provides ground point in the electrochemical cell, acts as a Faraday shield, and safeguards the set up during any surge of excessive electrical charges.

In three electrode systems, Ag/AgCl, Platinum, and active (synthesized) material is taken as reference, counter, and working electrode, respectively. In two electrode systems, the reference and counter leads are connected to one electrode of the supercapacitor, and the other electrode is connected to working and sense electrode lead. The desired electrical connections of three and two electrode systems have been shown in figure 3.12 (a) and (b).

Note: During the electrochemical characterizations, the working electrode potential is measured versus the reference electrode (here, Ag/AgCl) and the counter electrode (here, platinum) is used to complete the electrical circuit through which current flows.

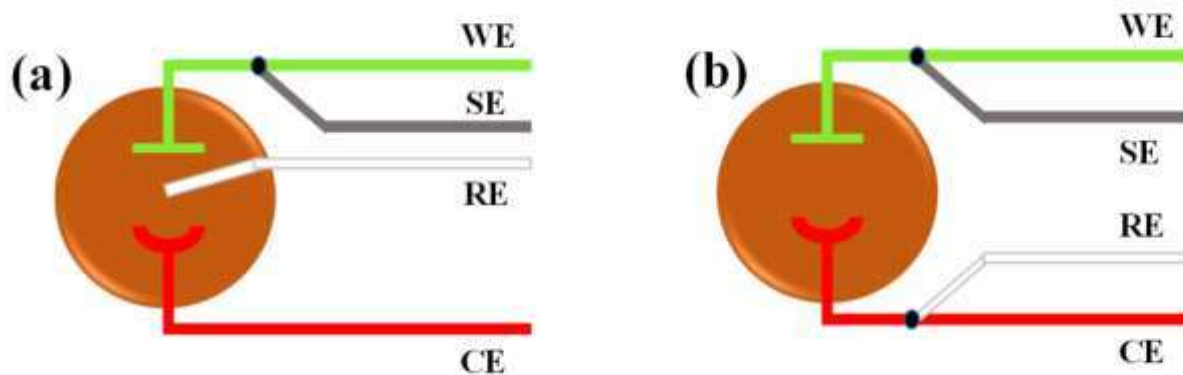


Figure 3.12: (a) Three electrode and (b) two electrode cell configurations

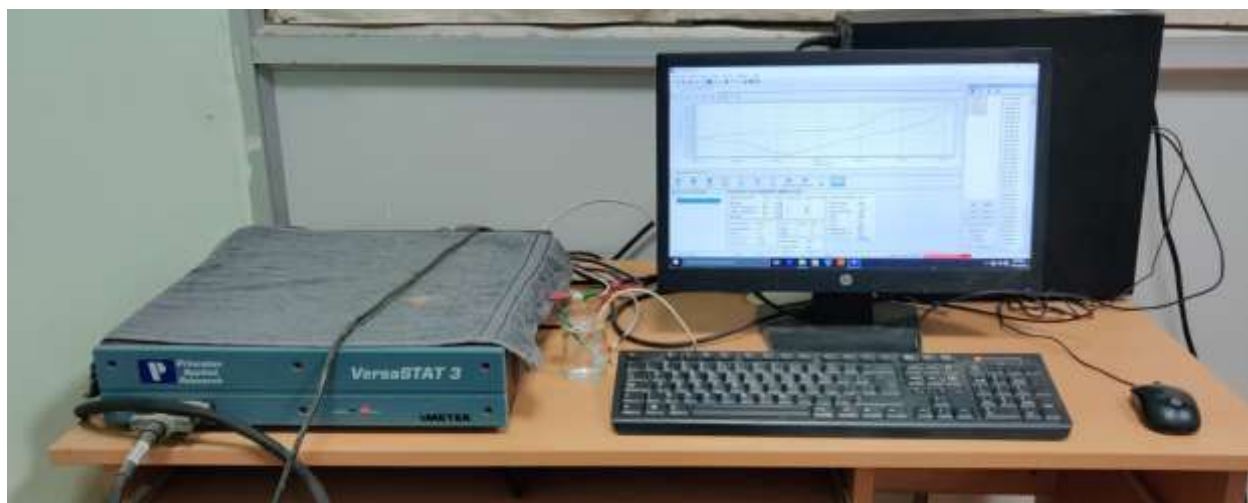


Figure 3.13: Experimental set-up used in the laboratory for electrochemical characterization

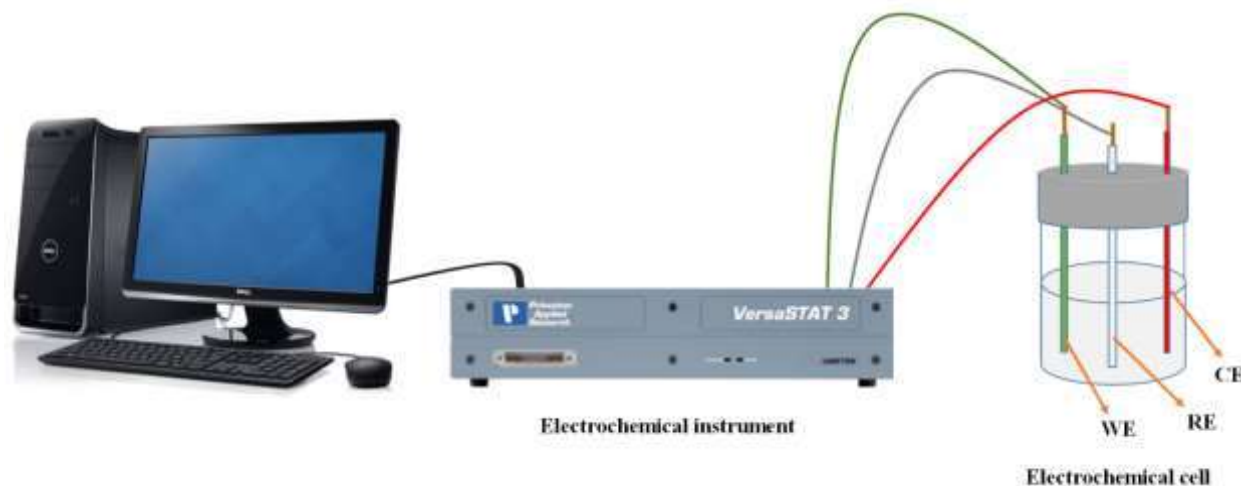


Figure 3.14: Schematic diagram of experimental set-up

3.2.8.4.1. CV

CV is a potentiodynamic electrochemical technique in which a potential is applied (stability potential window of the system) at a particular potential scan rate and current is generated as per the conductivity of the material used in the working electrode. The forward (anodic) and backward (cathodic) scan complete a cycle and the trace is known as cyclic voltammetry curve. The potential is applied between working and reference electrode, and the current is measured between working and counter electrode [199]. EDLC based materials like activated carbon, CNT, graphene oxide, etc. exhibit rectangular type CV. Pseudocapacitive materials like metal oxides (MnO_2 , RuO_2 , CuCo_2O_4 , CoFe_2O_4 , etc.), and conducting polymers (polyaniline, polythiophene, polypyrrole, etc.) exhibit redox transitions, and the CV curve has two regimes: capacitive regime which is dominated by double layer formation, and a faradaic regime that is prevailed by faradaic reactions [83].

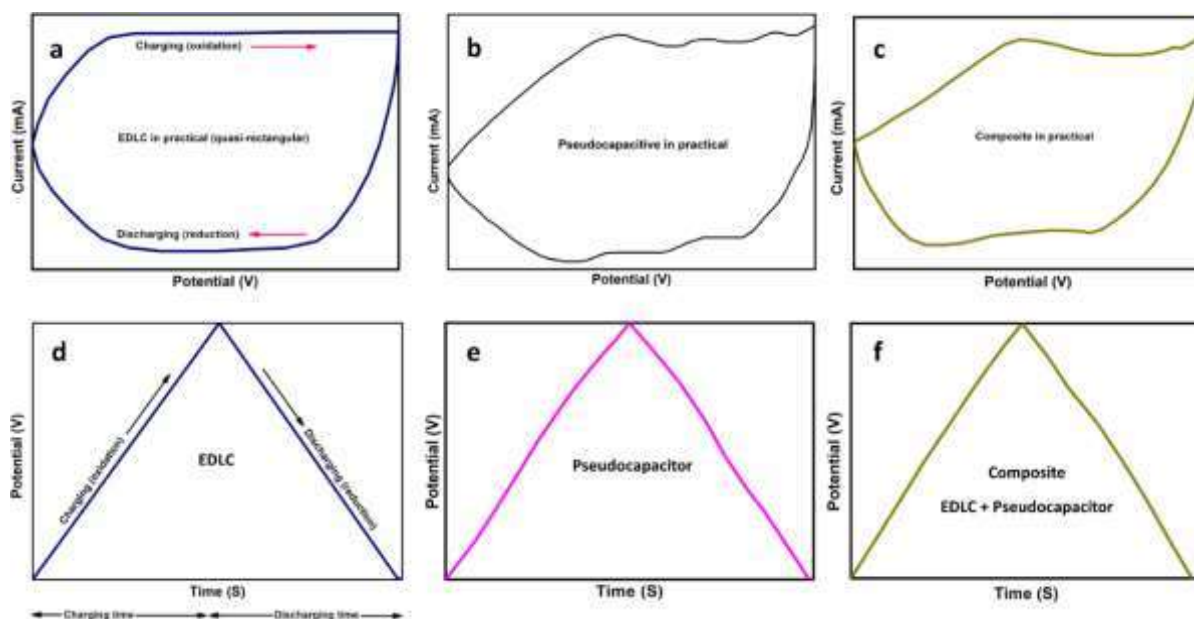


Figure 3.15: Sample CV and CD plot

Figure 3.15 a,b,c represent the cyclic voltammetry plot of EDLC, pseudocapacitive, composite material, respectively. The CV plot of an ideal capacitor is rectangular in nature. But, the deviation from rectangular shape in EDLC and pseudocapacitive material based supercapacitor could be due to the presence of functional groups and redox transitions, respectively. In case of composite material based supercapacitors, both the EDLC and pseudocapacitive materials may contribute significantly to get an enhanced electrochemical property [200,201]. The specific capacitance can be calculated using the following formulae.

Specific capacitance from CV

$$C_{sp,ele} = \frac{\int I * dV}{m_{ele} * v * \Delta V} \quad (3.5)$$

$C_{sp,ele}$ = Specific capacitance of a single electrode in Farad per gram (F/g)

$\int I * dV$ = Area under the cathodic scan in Ampere.Volt (AV)

m_{ele} = mass of the active material in gram (g)

v = Potential scan rate in volt per second (V/s)

ΔV = Stability potential window in volt (V)

Equation 3.5 can also be written as:

$$C_{sp,ele} = \frac{\int I * dV}{2 * m_{ele} * v * \Delta V} \quad (3.6)$$

In equation 3.6, $\int I * dV$ is the area under the whole CV curve. Factor '1/2' is included so as to correctly calculate the specific capacitance without overestimating the values.

Likewise,

$$C_{sp,sup} = \frac{\int I * dV}{m_{tot} * v * \Delta V} \quad (3.7)$$

$C_{sp,sup}$ = Specific capacitance of the supercapacitor (F/g)

$\int I * dV$ = Area under the cathodic scan (AV)

m_{tot} = total mass of the active material (g) = $m_{positive\ electrode} (m_{pe}) + m_{negative\ electrode} (m_{ne})$

3.2.8.4.2. CD

In CD technique, a constant current is applied during the process and the change in voltage of the supercapacitor with time is recorded. This is the most efficient technique for evaluation of capacitance. In EDLC, the potential window range is not restricted to a particular value as the charge storage is independent of potential. But for simple faradaic and intercalated pseudocapacitors, the range of potential window is fixed. In general, the CD plots of EDLCs are linear and triangular in shape, whereas for pseudocapacitors we get distorted CD plots with significant or negligible voltage drop. The charging and discharging time represent the response of a supercapacitor during any operation. Figure 3.15 d,e,f represent the charging-discharging plot of EDLC, pseudocapacitive, composite material,

respectively. The CD plot of an ideal capacitor is triangular in nature. But one may observe deviation from triangular shape due to functional groups in EDLC and redox reactions in pseudocapacitors. In case of composite systems, the deviation appears due to the presence of both type materials (EDLC and pseudocapacitive).

Specific capacitance can be calculated from the data obtained in CD.

$$C_{sp,ele} = \frac{I * t_d}{m_{ele} * \Delta V} \quad (3.8)$$

I = Discharging current (A)

t_d = Discharging time (s)

Likewise,

$$C_{sp,sup} = \frac{I * t_d}{m_{tot} * \Delta V} \quad (3.9)$$

There are various expressions for different types of configurations. For two equivalent electrodes having same capacitance and weight (symmetric systems), $C_{positive} = C_{negative}$.

$C_{positive}$ (C_{pe}) = Capacitance of positive electrode (pe)

$C_{negative}$ (C_{ne}) = Capacitance of negative electrode (ne)

Specific energy and power

Energy density is the amount of charge a supercapacitor can hold. It is directly proportional to the capacitance and square of the potential difference between the supercapacitor electrodes.

Equation for specific energy,

$$E_{sp,sup} = \frac{1}{2} * C_{sp,sup} * (\Delta V)^2 \quad (3.10)$$

$E_{sp,sup}$ = Specific energy of the supercapacitor in Watt-hour per kilogram (Wh/kg)

Power density is the rate at which a device delivers the stored energy during an application.

$$P_{sp,sup} = \frac{E_{sp,sup}}{t_d} \quad (3.11)$$

$P_{sp,sup}$ = Specific power of the supercapacitor (W/kg)

t_d = Discharging time of the supercapacitor (s)

Coulombic efficiency (η)

Coulombic efficiency demonstrates the efficiency at which charges (electrons) are transferred in an electrochemical system during the operation of the device. It is also called as current efficiency or faradaic efficiency.

$$\eta \% = \frac{t_d}{t_c} * 100 \quad (3.12)$$

η % = Percentage coulombic efficiency (CE)

t_d = Discharging time of the supercapacitor (s)

t_c = Charging time of the supercapacitor (s)

Cycle life

The reliability of a supercapacitor is estimated from its percentage retention over repeated cycles of charge-discharge or cyclic voltammetry. Supercapacitors exhibit excellent capacitance retention and higher cycle life than batteries and fuel cells.

3.2.8.4.3. EIS

It is well knowing that electrical resistance is the opposition provided by a circuit element to the flow of electrical current. An ideal resistor follows Ohm's law ($V=IR$) at all voltage and current levels, its resistance does not depend on frequency, and AC voltage and current through such resistors lie in phase with each other. In real applications, the circuit elements display complex behavior and they do not allow us to implement the general concepts of resistance. So, we use a more generalized term i.e., impedance. Like resistance, it is also the

measure of the obstruction offered by a circuit element [142,202,203]. In supercapacitor applications, the impedance is measured by EIS technique.

According to Ohm's law,

$$V \propto I$$

$$\Rightarrow V = IR \quad (3.13)$$

V is the potential in volt (V), I is the current in Ampere (A), and R is the resistance in Ohm (Ω).

Equation 3.23 is applicable to ideal resistors. An ideal resistor holds the following properties.

- (a) Ohm's law is applicable at all voltage and current.
- (b) The resistance is frequency independent.
- (c) In case of a resistor, AC voltage and current are in phase.

According to Euler's formula,

$$\exp(j\phi) = \cos \phi + j \sin \phi$$

The impedance can be expressed in the form of a complex function.

$$V_X = |V_0| \exp(j\omega t)$$

$$I_X = |I_0| \exp(j\omega t - \phi)$$

$$j = \sqrt{-1}$$

$$Z = |Z_0| \exp(j\phi) = |Z_0| (\cos \phi + j \sin \phi) = |Z_0| \cos \phi + j |Z_0| \sin \phi = Z_{Re} + j Z_{Im}$$

$$|Z| = \sqrt{Z_{Re}^2 + Z_{Im}^2} \quad (3.14)$$

$|Z|$ = Total impedance in Ohms (Ω)

Z_{Re} = Real part of impedance (Ω)

Z_{Im} = Imaginary part of impedance (Ω)

An AC amplitude is given to the cell during the EIS process over a frequency range of 100 mHz to 1 MHz. Various plots like Nyquist plot (Z_{re} vs Z_{im}) and Bode plot (frequency vs $|Z|$) are obtained from the EIS data. The point at which the extrapolated plot intersects the real axis at high frequency region, is known as equivalent series resistance (R_{eq}). It is the collective resistances of current collector, substrate, electrolyte, etc. The diameter of the semicircle in the Nyquist plot demonstrates charge transfer resistance (R_{ct}). The absence of any semicircle represents ultralow charge transfer resistance. Less charge transfer resistance value signifies excellent electron and ion mobility, which enhances the charge-discharge rate of the system [204]. A typical Nyquist plot has been given in figure 3.16.

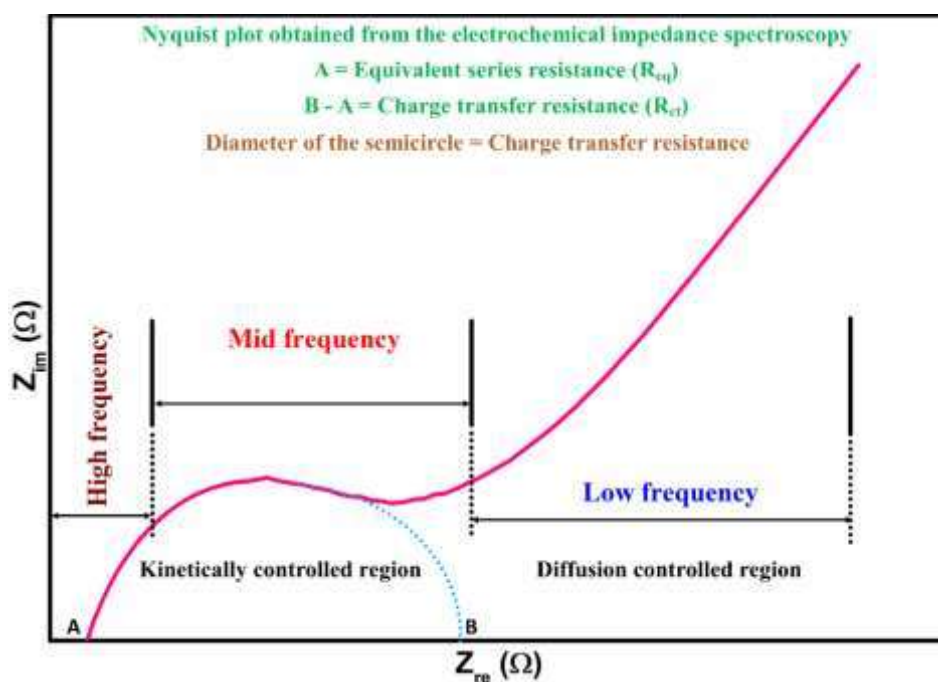


Figure 3.16: Sample EIS plot

Point 'A' (beginning of the semicircle corresponding to the intercept on real z axis) in figure 3.16 represents the equivalent series resistance of the system. Diameter of the semicircle (B-A) resembles the charge transfer resistance (R_{ct}) which is the measure of resistance

encountered during the flow of electrons through the system. The straight line in the low frequency region is attributed to the Warburg diffusion resistance which is the resistance offered to the electrolyte ions when they diffuse through the bulk and electrode material [205]. The main goal of this research is to create hybrid systems and composite materials in order to obtain improved electrochemical characteristics.

